EDN: GDTCRO
УДК 541.122: 538.214

NEXAFS and XPS Spectra of Mn Doped Bismuth Magnesium Tantalate Pyrochlores

Nadezhda A. Zhuk*
Pitirim Sorokin Syktyvkar State University
Syktyvkar, Russian Federation
Sergey V. Nekipelov†
Institute of Physics and Mathematics of the Komi Science Center UB RAS
Syktyvkar, Russian Federation
Alexandra V. Koroleva‡
Saint Petersburg State University
St. Petersburg, Russian Federation
Alexey M. Lebedev§
National Research Center – Kurchatov Institute
Moscow, Russian Federation
Dmitriy S. Beznosikov¶
Federal State Unitary Enterprise «General Radio Frequency Centre»
Syktyvkar, Russian Federation

Received 10.03.2024, received in revised form 15.04.2024, accepted 17.05.2024

Abstract. According to X-ray powder phase analysis, $Bi_2Mg_xMn_{1-x}Ta_2O_{9.5-\Delta}$ (x=0.3;0.5;0.7) samples synthesized using ceramic technology contain the main phase of cubic pyrochlore (space group Fd-3m) and the impurity phase $BiTaO_4$ of the triclinic modification (sp. Gr. P-1), the content of which is proportional to the degree of doping with manganese. The unit cell parameter of the pyrochlore phase increases uniformly with increasing index x(Mg) from 10.4970(8) at x=0.3 to 10.5248(8) Å (x=0.7), obeying the Vegard rule. The electronic state of all ions included in $Bi_2Mg_xMn_{1-x}Ta_2O_{9.5-\Delta}$ was studied using X-ray spectroscopy. According to NEXAFS and XPS data, it was established that doping with magnesium does not change the oxidation state of bismuth and tantalum in pyrochlore. Meanwhile, in the Ta4f$_-$, Bi4f$_{7/2}$ and Bi4$_{f5/2}$ spectra of the samples, an energy shift of the absorption bands towards lower energies is observed, which is typical for bismuth and tantalum ions with an effective charge of (+3-δ) and (+5-δ), caused by the distribution of manganese(II) and magnesium(II) ions in the position of bismuth and tantalum. According to NEXAFS and XPS spectroscopy, manganese ions in the samples have oxidation states predominantly +2 and +3, the proportion of which increases with increasing manganese content in the samples.

Keywords: pyrochlore, Zn,Mg doping, $BiTaO_4$, XPS and NEXAFS spectroscopy.

Citation: N.A. Zhuk, S.V. Nekipelov, A.V. Koroleva, A.M. Lebedev, D.S. Beznosikov, NEXAFS and XPS Spectra of Mn Doped Bismuth Magnesium Tantalate Pyrochlores, J. Sib. Fed. Univ. Math. Phys., 2024, 17(4), 544–553. EDN: GDTCRO.

*nzhuck@mail.ru
†nekipelovsv@mail.ru
‡dalika@inbox.ru
§lebedev.alex.m@gmail.com
¶uvn71p3@gmail.com

Due to their excellent dielectric properties, the ability to regulate dielectric properties by an electric field, low sintering temperature and chemical compatibility with low-melting Ag, Cu conductors, oxide pyrochlores are promising as dielectrics for multilayer ceramic capacitors, tunable microwave dielectric components, resonators, devices for microwave applications [1–4]. Materials based on pyrochlores are used in solid-state devices as thin-film resistors, thermistors and communication elements, photocatalysts, and are used as components of ceramic molds for radioactive waste. The formula of oxide pyrochlores $A_2B_2O_7$ describes a large family of compounds isostructural with the mineral pyrochlore. In the crystal structure of pyrochlore, two cationic sublattices with the anticristobalite structure A_2O' and the octahedral B_2O_6 are distinguished [5]. The positions of cations A with octaoxygen coordination are occupied by large ions (Ca^{2+}, Bi^{3+}). The three-dimensional framework of B_2O_6 is formed by [BO_6] octahedra connected at the vertices, in the positions of which cations with a smaller ionic radius (Ti^{4+}, Ta^{5+}) are located. There are known cases of mixed pyrochlores with three or more types of cations located at two nonequivalent cation positions A and B. These include pyrochlores based on bismuth tantalate, doped with ions of 3d elements [6, 7]. Such doping options lead to the formation of a pyrochlore structure deficient in cations A, as is typical for bismuth-containing pyrochlores and is the reason for the relaxation properties of oxide ceramics. Currently, almost all pyrochlores based on bismuth tentalate containing 3d ions (Cr,Fe,Co,Ni,Cu,Zn) are known and studied. Due to their excellent dielectric properties, such pyrochlores are promising as multilayer ceramic capacitors, resistors, resonators, sensors and microwave filters [3, 4]. As shown in [8], iron-containing pyrochlores $Bi_{3.36}Fe_{2.08+x}Ta_{2.56-x}O_{14.56-x}$ ($-0.32 \leqslant x \leqslant 0.48$) exhibit moderate values of dielectric constant $\varepsilon \sim 78-92$ and dielectric loss tangent $\delta \sim 10^{-1}$ at 30 °C and 1MHz. Magnesium-containing pyrochlores $Bi_{3+5/2x}Mg_{2-x}Ta_{3-3/2x}O_{14-x}$ ($0.12 \leqslant x \leqslant 0.22$) are characterized by comparable values of $\varepsilon \sim 70-85$ and low dielectric loss tangent $\delta \sim 10^{-3}$ at 1 MHz and 30 °C [9]. For pyrochlore $Bi_{1.5}ZnTa_{1.5}O_7$, the dielectric constant is close to 58 [10]. We have not found any information on manganese-containing pyrochlores based on bismuth tantalate. There is one known work devoted to the study of analog pyrochlores in the Bi_2O_3-Mn_2O_3-Nb_2O_5 system [7]. The authors of the article found that a significant concentration region of bismuth-deficient manganese-containing pyrochlores is formed in the system, in which 14 – 30% of the A-positions are occupied by Mn^{2+} ions. As the authors of [7] showed, X-ray powder diffraction data confirmed that all Bi-Mn-Nb-O pyrochlores form with structural displacements, as found for the analogous pyrochlores with Mn replaced by Zn, Fe, or Co. According to [7], the displacive disorder is crystallographically analogous to that reported for $Bi_{1.5}Zn_{0.92}Nb_{1.5}O_{6.92}$, which has a similar concentration of small B-type ions on the A-sites. EELS spectra of manganese-containing pyrochlores showed the presence of Mn^{2+} and Mn^{3+} ions. Manganese in high-temperature ceramics can have a complex ionic composition, affecting the physicochemical properties of the ceramics. The ionic state of manganese is influenced by many variable factors, among which the symmetry and strength of the crystal field, the nature of the ligands, distortions and the size of the coordination polyhedron are particularly prominent. Studies have shown that the combined use of X-ray spectroscopy methods (XPS, NEXAFS) makes it possible to most accurately determine the ionic composition of complex oxides [11]. As part of our work, we studied the electronic state of manganese ions in Mg and Mn codoped bismuth tantalate pyrochlores using NEXAFS and XPS spectroscopy. The influence of the degree of substitution of Ta(V) ions on the proportion of oxidized manganese ions in pyrochlores has been established.

1. Materials and methods

$Bi_2Mg_xMn_{1-x}Ta_2O_{9.5-\Delta}$ (x=0.3,0.5,0.7) samples were synthesized using the solid-phase reaction method from the oxides MgO, Bi_2O_3, Mn_2O_3, Ta_2O_5. A finely ground and homogeneous stoichiometric mixture of oxides was pressed into disc-shaped compacts (diameter 10 mm, thickness 3 – 4 mm) using a hand press. High-temperature treatment of the samples was carried out in stages, at temperatures of 650, 850, 950, 1050 °C for 15 hours at each calcination stage. The phase composition was determined by X-ray phase analysis using a Shimadzu 6000 X-ray diffractometer (CuKα radiation). The microstructure and local elemental composition of the samples were studied using scanning electron microscopy and energy-dispersive X-ray spectroscopy (electron scanning microscope Tescan VEGA 3LMN, energy dispersion spectrometer INCA Energy 450). XPS studies were carried out using the equipment of the resource center of the Science Park of St. Petersburg State University "Physical methods of surface research." XPS analysis was performed on a Thermo Scientific ESCALAB 250Xi X-ray spectrometer. An X-ray tube with AlKα radiation (1486.6 eV) was used as a source of ionizing radiation. To neutralize the sample charge in the experiments, an ion-electronic charge compensation system was used. All peaks were calibrated relative to the C1s peak at 284.6 eV. Processing of experimental data was carried out using the software of the ESCALAB 250Xi spectrometer. The samples were studied using NEXAFS spectroscopy at the NanoPES station of the KISS synchrotron source at the Kurchatov Institute (Moscow) [11]. NEXAFS spectra were obtained by recording the total electron yield (TEY) with an energy resolution of 0.5 eV.

2. Results and discussion

2.1. Phase composition of the $Bi_2Mg_xMn_{1-x}Ta_2O_{9.5-\Delta}$

Based on X-ray powder phase analysis, it was established that samples of the composition $Bi_2Mg_xMn_{1-x}Ta_2O_{9.5-\Delta}$ (x = 0.3-0.7) are two-phase (Fig. 1). In addition to the main cubic phase, they contain bismuth orthotantalate $BiTaO_4$ of the triclinic modification (space group P-1) as an impurity [12]. Analysis of the reflection extinctions of the cubic phase established that the symmetry of the crystal structure is cubic with space group *Fd-3m* [5] and corresponds to the structure of cubic pyrochlore. The amount of bismuth orthotantalate is proportional to the content of manganese ions and varies from 7.9 (x(Mn)=0.3) to 23.8 wt.% (x(Mn)=0.7). The proportionality of the amount of impurity to the manganese content in the samples can mean the distribution of some manganese ions in the bismuth position, and magnesium ions in the octahedral positions of tantalum(V), as shown earlier using the example of solid solutions $Bi_2Mg_xM_{1-x}Ta_2O_{9.5-\Delta}$ (M-Ni,Cr, Fe) [13–15]. The appearance of impurities in the samples may be associated with the placement of Mn(II) ions not only in the octahedral sublattice of tantalum(V), but also in the bismuth(III) sublattice, which is due to the larger sizes of Mn(II) ions than those of Mg(II), similar behavior was observed for cobalt(II) ions [16]. Apparently, when doped with large manganese ions, most of them are distributed into the octahedral sublattice of tantalum(V), creating oxygen vacancies and thereby causing stress in the octahedral framework as a whole. In order to relieve stress in the crystal structure, some manganese(II) ions are placed in the bismuth(III) position. The system responds to this placement by creating vacancies in the bismuth sublattice by releasing a bismuth orthotantalate phase as an impurity. The amount of bismuth orthotantalate impurity is equivalent to the number of 3d ions located in the bismuth position [16]. The unit cell parameter of cubic pyrochlore in $Bi_2Mg_xMn_{1-x}Ta_2O_{9.5-\Delta}$ decreases

uniformly with an increase in the content of manganese ions (and a decrease in magnesium ions) in the samples from 10.5248(8) (x(Mn)=0.3) to 10.4970(8) Å (x(Mn)=0.7), despite the fact that the ionic radius of magnesium(II) is smaller than the radius of Mn(II) ions (R(Mg(II))c.n-6=0.72 Å, R(Mn(II))c.n-6=0.83 Å), but more than tantalum(V) ions (R(Ta(V))c.n-6=0.64 Å) [17]. The increase in the unit cell parameter with an increase in magnesium ions can be explained by the fact that with increasing magnesium content the amount of impurity decreases, which means the pyrochlore cell parameter is higher, and also by the fact that Mn(II) ions can occupy bismuth(III) positions, the ionic radius of which less than bismuth(III) ions (R(Bi(III))c.n-8=1.17 Å, R(Mn(II))c.n-8=0.90 Å) [17], and do not make a significant contribution to the cell parameter. In this regard, the cell parameter increases due to the distribution of large magnesium(II) ions into the octahedral positions of tantalum(V).

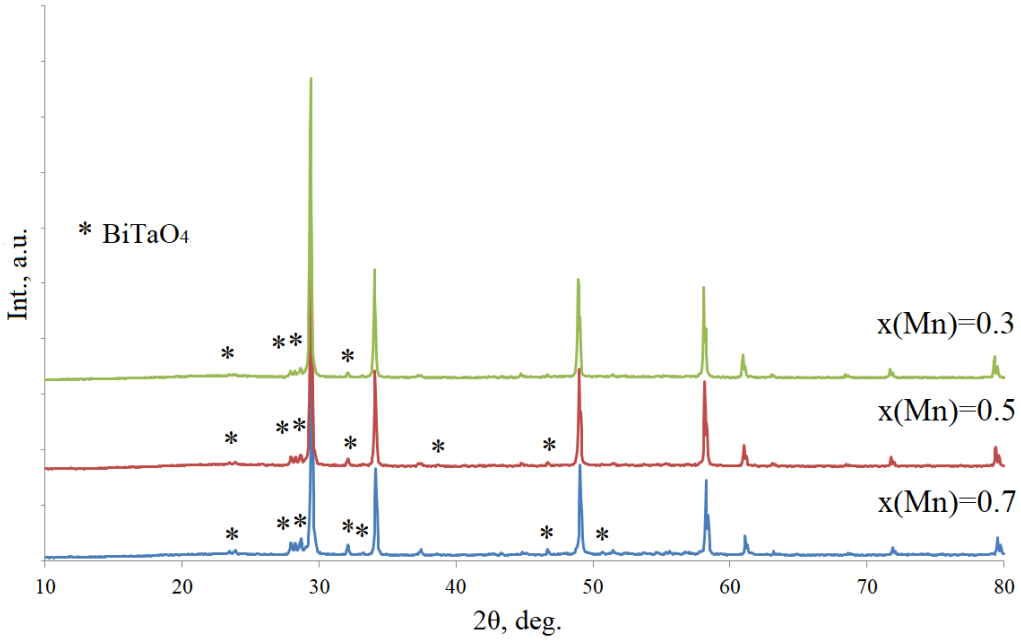

Fig. 1. X-ray powder diffraction patterns of $Bi_2Mg_xMn_{1-x}Ta_2O_{9.5-\Delta}$ samples with varying index x(Mn)

2.2. XPS and NEXAFS spectra of the $Bi_2Mg_xMn_{1-x}Ta_2O_{9.5-\Delta}$

The obtained XPS spectra of magnesium bismuth tantalate $Bi_2Mg_xMn_{1-x}Ta_2O_{9.5-\Delta}$ are presented in Fig. 2. The energy position of the details of the spectra are presented in Tab. 1. For comparison, the spectra of the original oxides used in the synthesis of the samples are given. Fig. 2 shows XPS spectra in a wide energy range and spectral dependences in the region of the Bi5d-, Ta4f-, Ta4d- and Mn2p-ionization thresholds of the studied samples. The figures also show the results of decomposing the spectral dependences into individual peaks, which were modeled by Gaussian-Lorentzian curves, and the background lines by the Shirley or smart approximation. When analyzing the Survey XPS spectrum, one can note the presence of a C1s peak associated with the presence of contaminants on the surface, which cannot be removed from the surface

of the sample. In this regard, a contribution to the intensity of the O1s peak from surface contaminants is possible. Thus, to analyze the surface composition of samples, which manifests itself in XPS spectra, it is possible only on the basis of analysis of the spectra of bismuth, tantalum and manganese.

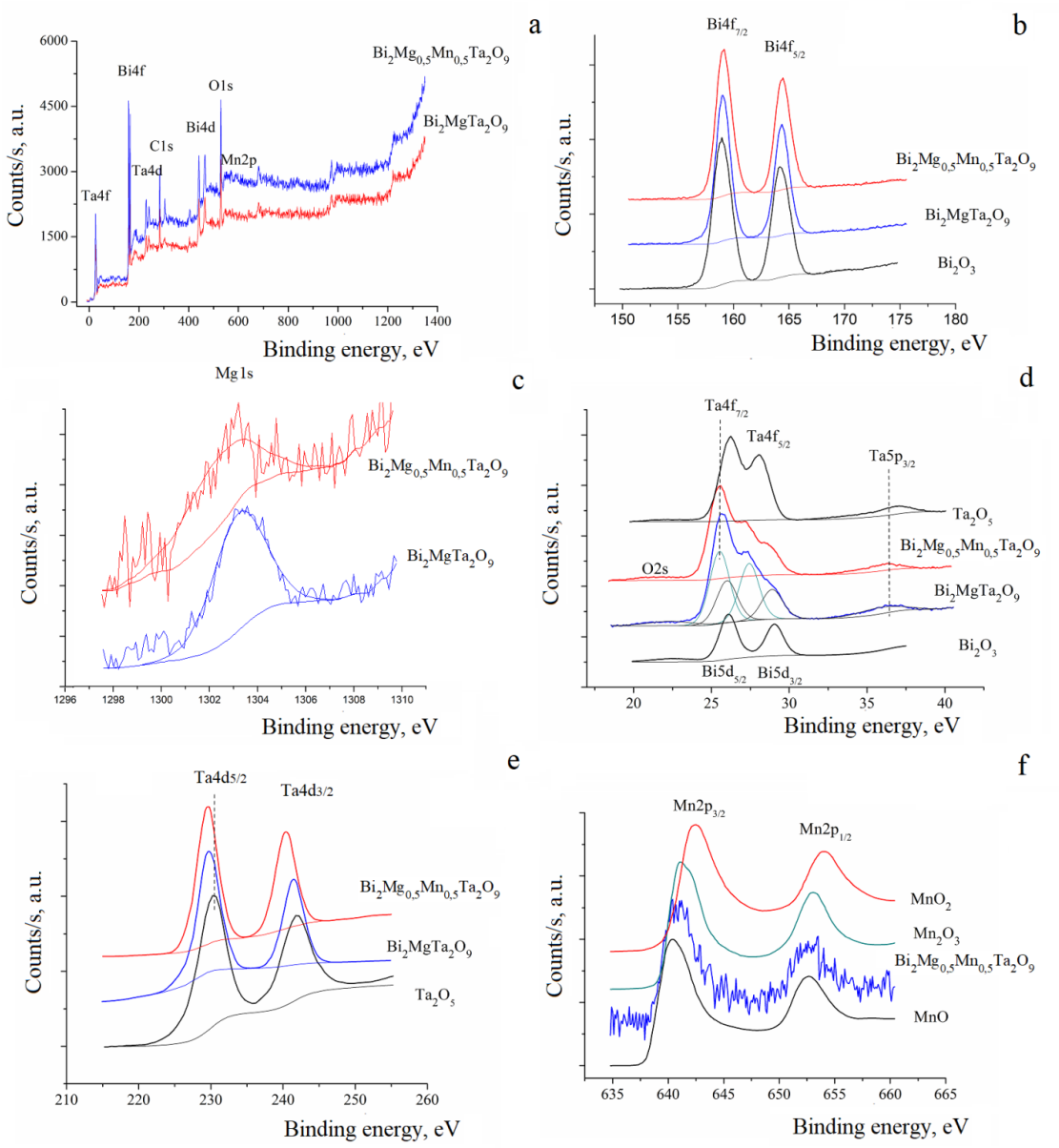

Fig. 2. Survey XPS spectra of $Bi_2Mg_{0.5}Mn_{0.5}Ta_2O_{9.5-\Delta}$ and $Bi_2MgTa_2O_9$ (a), Bi4f spectra of bismuth atoms (b), Mg1s spectra (c), XPS spectra of tantalum and bismuth atoms (d), Ta4d- spectra (e), Mn2p spectra (f). For comparison, the spectra of MnO [18], Mn_2O_3 [19] and MnO_2 [20] are given

It should be noted that doping with manganese atoms practically does not change the spectral

characteristics of bismuth, tantalum and magnesium atoms (Fig. 2b-2e). When comparing the XPS Bi4f spectra of the sample under study and Bi_2O_3 oxide (Fig. 2b), it can be noted that the energy position and width of the peaks in the spectrum of the sample correlate with the corresponding spectra of Bi_2O_3 oxide. It is interesting to note that for the $Bi_2Mg_{0.5}Mn_{0.5}Ta_2O_{9.5-\Delta}$ sample there is a slight shift in the absorption bands of $Bi5d_{3/2}$, $Bi5d_{5/2}$, $Bi4f_{7/2}$ and $Bi4f_{5/2}$ compared to $Bi_2MgTa_2O_9$ to lower energies (from 164.12 eV ($Bi_2Mg_{0.5}Mn_{0.5}Ta_2O_{9.5-\Delta}$) to 164.35 eV $Bi_2MgTa_2O_9$), which means a decrease in the effective charge of bismuth ions. Apparently, the shift of the peaks is associated with the placement of a certain proportion of divalent ions, for example, manganese(II), in the bismuth position, as shown by X-ray phase analysis. The energy positions of the peaks in the XPS Mg1s spectra shown in Fig. 2c is typical for the divalent magnesium atom [21]. When considering the spectra of tantalum atoms (Fig. 2d, 2e), it should be noted that the shape of the peaks clearly indicates that all tantalum atoms are in the same charge state (there is no splitting or distortion of the peaks), but at the same time the energy position of the peaks has a characteristic shift in side of lower energies compared to the binding energy in pentavalent tantalum oxide Ta_2O_5. A shift towards lower energies is characteristic of a decrease in the effective positive charge; in particular, for the Ta4f and Ta5p spectra we presented, this energy shift is ΔE=0.7 eV, and in the region of the Ta4d edge - 1 eV. This in turn allows us to assume that tantalum atoms have the same effective charge +(5-δ), which we observed in similar spectra of tantalum in bismuth tantalates doped with Cr, Fe, Co, Ni, Cu atoms [13–16, 22]. Let's move on to consider the Mn2p spectra presented in Fig. 1f. Comparison of the spectra of the composite with the spectra of the oxides MnO [18], Mn_2O_3 [19] and MnO_2 [20] known from the literature shows that the spectrum of $Bi_2Mg_{0.5}Mn_{0.5}Ta_2O_{9.5-\Delta}$ correlates well with the spectrum of MnO, while the spectra of Mn_2O_3 and MnO_2 has a shift towards higher energies. All this suggests that magnesium atoms are mainly in the Mn+2 charge state in this composite.

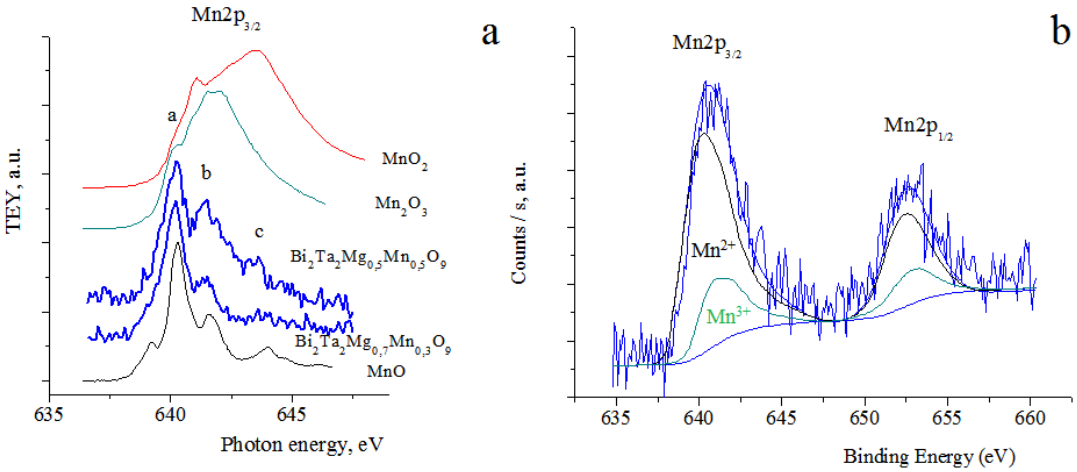

Fig. 3. NEXAFS Mn2p spectra in $Bi_2Mg_{0.5}Mn_{0.5}Ta_2O_{9.5-\Delta}$, $Bi_2Mg_{0.3}Mn_{0.7}Ta_2O_{9.5-\Delta}$, in MnO, Mn_2O_3 and MnO_2 oxides (a); decomposition of the XPS Mn2p spectrum of $Bi_2Mg_{0.5}Mn_{0.5}Ta_2O_{9.5-\Delta}$ into individual components (b)

Let us move on to consider the NEXAFS Mn2p spectra of the $Bi_2Mg_{0.5}Mn_{0.5}Ta_2O_{9.5-\Delta}$ and

$Bi_2Mg_{0.3}Mn_{0.7}Ta_2O_{9.5-\Delta}$ composites presented in Fig. 3a. When comparing the spectra of the composites with the spectra of the oxides we obtained, it can be noted that the shape of the spectra and the energy position of the main peaks (a-c) in all of the given spectra of the composite coincide well with the spectra of MnO. This suggests that the manganese atoms in the studied samples mainly have a charge state of +2. It should be noted that the c band, which can be identified as a separate peak in the spectrum of MnO, is visible in the spectra of the composites as an influx. In addition, in the spectra of composites, compared to the spectrum of MnO, the relative intensity of the b bands also increases. Beam c coincides in energy position with a broad band in the spectrum of MnO_2, and bands a and b correlate well with the corresponding features in the spectra of Mn_2O_3, but with different intensities. This suggests that the manganese atoms in the composites are both in the charge state +2 and partially +3/+4.

To clarify this conclusion, we attempted to decompose the XPS Mn2p spectra of the $Bi_2Mg_{0.5}Mn_{0.5}Ta_2O_{9.5-\Delta}$ sample into individual components, using the spectra of the oxides presented in Fig. 3b. The decomposition was carried out according to the following procedure: (1) background lines obtained using the Shirley approximation were subtracted from the spectra, (2) "background-free" XPS spectra obtained in this way were normalized by area by one value (in this case, 1 was taken), (3) a model spectrum was constructed as the sum of the XPS spectra of MnO, Mn_2O_3 and MnO_2 with the corresponding coefficients α, β and γ ($\alpha+\beta+\gamma = 1$), the value of which was varied to achieve maximum agreement with the spectrum of the composite. The Fisher F-criterion was taken as a criterion for optimal agreement for the considered intensities of the XPS spectra of the composite and the model spectrum. The results of optimal modeling are presented in Fig. 3, for which $\alpha = 0.77$, $\beta = 0.23$ and $\gamma = 0$ (Fisher's F test is 0.9998). The data obtained in this way suggests that in the structure of the $Bi_2Mg_{0.5}Mn_{0.5}Ta_2O_{9.5-\Delta}$ composite there are two nonequivalent states of manganese atoms: about 77% of manganese atoms are in the +2 charge state, and the remaining 23% are in +3. Turning again to the NEXAFS spectra (Fig. 3a), we can assume that the presence of an intense b band indicates the presence of Mn^{3+} ions in the composite. Moreover, with increasing manganese content in $Bi_2Mg_xMn_{1-x}Ta_2O_{9.5-\Delta}$, (x=0.5 and 0.3), the intensity of this peak increases, which is an indication of an increase in the proportion of Mn^{3+} ions in the samples and is consistent with the quantitative assessment of the proportion of manganese ions according to XPS analysis.

Table 1. Energy positions of the components of the XPS spectra of $Bi_2Mg_{0.5}Mn_{0.5}Ta_2O_{9.5-\Delta}$ (1) and $Bi_2MgTa_2O_9$ (2)

Peak	Energy (eV)	
	1	2
$Bi4f_{7/2}$	158.80	159.03
$Bi4f_{5/2}$	164.12	164.35
$Bi5d_{5/2}$	25.82	26.11
$Bi5d_{3/2}$	28.72	29.08
$Ta4f_{7/2}$	25.31	25.66
$Ta4f_{5/2}$	27.21	27.56
$Ta4d_{5/2}$	229.49	229.78
$Ta4d_{3/2}$	240.32	241.44
Mg1s	1302.49	1303.19
$Mn2p_{3/2}$	640.83	
$Mn2p_{1/2}$	652.39	

Conclusions

The $Bi_2Mg_xMn_{1-x}Ta_2O_{9.5-\Delta}$ composites were synthesized by the solid-phase method and, according to X-ray diffraction data, contain $BiTaO_4$ impurity, the content of which in the samples increases with increasing index x(Mn). The unit cell parameter of the pyrochlore phase increases with increasing magnesium content in the samples. The appearance of bismuth orthotantalate impurities is associated with the distribution of some manganese ions into the bismuth cation sublattice. This assumption is confirmed by the energy shift to lower energies of the bismuth absorption bands ($Bi4f_{7/2}$ and $Bi4f_{5/2}$). According to NEXAFS and XPS data, it was established that bismuth and magnesium ions are in the charge states Bi(+3-δ), Zn(+2). Based on the characteristic shift of the absorption band in the Ta4f spectrum to lower energies, it was established that tantalum ions have an oxidation state of Ta(+5-δ). It has been shown that doping pyrochlores with manganese and magnesium ions leads to the oxidation of some manganese ions to Mn(III), the proportion of which increases with increasing manganese content in the samples.

The authors thank the X-ray Diffraction Center SPSU for providing instrumental and computational resources. The XPS studies were performed on the equipment of the Resource Center "Physical methods of surface investigation" of the Scientific Park of St. Petersburg University. The NEXAFS studies were performed on the synchrotron radiation from station "NanoPES" storage ring (National Research Center "Kurchatov Institute"). The study was supported by the Ministry of Science and Higher Education of Russia under Agreement no. 075-15-2021-1351 in part of NEXAFS research.

References

[1] Z.Hiroi, J.-I.Yamaura, Y S.onezawa, H.Harima, Chemical trends of superconducting properties in pyrochlore oxides, *Physica C: Superconductivity and Appl.*, **460-462**(2007), 20–27. DOI: 10.1016/j.physc.2007.03.023

[2] P.F.ABongers, E.R.Meurs, Ferromagnetism in Compounds with Pyrochlore Structure, *J. Appl. Phys.*, **38**(1967), 944–945.

[3] H.Du, X.Yao, Structural trends and dielectric properties of Bi-based pyrochlores, *J. Mater. Sci. Mater. Electron.*, **15**(2004), 613–616. DOI: 10.1023/B:JMSE.0000036041.84889.b2

[4] C.C.Khaw, K.B.Tan, C.K.Lee, High temperature dielectric properties of cubic bismuth zinc tantalite, *Ceram. Intern.*, **35**(2009), 1473–1480. DOI: 10.1016/j.ceramint.2008.08.006

[5] R.A.McCauley, Structural Characteristics of Pyrochlore Formation, *J. Appl. Phys.*, **51**(1980), 290–294.

[6] T.A.Vanderah, T.Siegrist, M.W.Lufaso, M.C.Yeager, R.S.Roth, J.C.Nino, S.Yates, Phase Formation and Properties in the System Bi_2O_3:$2CoO_{1+x}$:Nb_2O_5, *Eur. J. Inorgan. Chem.*, **2006**(2006), 4908–4914. DOI: 10.1002/EJIC.200600661

[7] T.A.Vanderah, M.W.Lufaso, A.U.Adler, I.Levin, J.C.Nino, V.Provenzano, P.K.Schenck, Subsolidus phase equilibria and properties in the system Bi_2O_3:Mn_2O_3±x:Nb_2O_5, *J. Sol. St. Chem.*, **179**(2006), 3467–347. DOI: 10.1016/J.JSSC.2006.07.014

[8] F.A.Jusoh, T K.B.an, Z Z.ainal, S.K.Chen, C.C.Khaw, O.J.Lee, Novel pyrochlores in the Bi_2O_3-Fe_2O_3-Ta_2O_5 (BFT) ternary system: synthesis, structural and electrical properties, *J. Mater. Res. Techn.*, **9**(2020), 11022–11034. DOI: 10.1016/j.jmrt.2020.07.102

[9] P.Y.Tan, K.B.Tan, C.C.Khaw, Z.Zainal, S.K.Chen, M.P.Chon, Phase equilibria and dielectric properties of $Bi_{3+(5/2)x}Mg_{2-x}Nb_{3-(3/2)x}O_{14-x}$ cubic pyrochlores, *Ceram. Intern.*, **40**(2014), 4237–4246.

[10] C.C.Khaw, K.B.Tan, C.K.Lee, A.R.West, Phase equilibria and electrical properties of pyrochlore and zirconolite phases in the Bi_2O_3-ZnO-Ta_2O_5 system, *J. Eur. Ceram. Soc.*, **32**(2012), 671–680. DOI: 10.1016/j.jeurceramsoc.2011.10.012

[11] A.M.Lebedev, K.A.Menshikov, V.G.Nazin, V.G.Stankevich, Tsetlin M.B., Chumakov R.G., NanoPES Photoelectron Beamline of the Kurchatov Synchrotron Radiation Source, *J. Surface Investigation: X-ray, Synchrotron and Neutron Techniques*, **15**(2021), 1039–1044. DOI: 10.1134/S1027451021050335

[12] N.A.Zhuk, M.G.Krzhizhanovskaya, V.A.Belyy, V.V.Kharton, Chichineva A.I., Phase transformations and thermal expansion of α- and β-$BiTaO_4$ and the high-temperature modification γ-$BiTaO_4$, *Chem. Mater.*, **32**(2020), 5943–5501. DOI: 10.1021/acs.chemmater.0c00010

[13] Z N.A.huk, K M.G.rzhizhanovskaya, A.V.Koroleva, etc., Fe,Mg-Codoped Bismuth Tantalate Pyrochlores: Crystal Structure, Thermal Stability, Optical and Electrical Properties, XPS, NEXAFS, ESR, and ^{57}Fe Mössbauer Spectroscopy Study, *J. Mater. Res.*, **11**(2023), 8. DOI: 10.3390/inorganics11010008

[14] N.A.Zhuk, M.G.Krzhizhanovskaya, N.A.Sekushin, V.V.Kharton, etc., Novel Ni-Doped Bismuth–Magnesium Tantalate Pyrochlores: Structural and Electrical Properties, Thermal Expansion, X-ray Photoelectron Spectroscopy, and Near-Edge X-ray Absorption Fine Structure Spectra, *ACS Omega*, **6**(2021), 23262–23273. DOI: 10.1021/acsomega.1c02969

[15] N.A.Zhuk, M.G.Krzhizhanovskaya, A.V.Koroleva, etc., Cr and Mg codoped bismuth tantalate pyrochlores: Thermal expansion and stability, crystal structure, electrical and optical properties, NEXAFS and XPS study, *J. Sol. St. Chem.*, **323**(2023) 124074. DOI: 10.1016/j.jssc.2023.124074

[16] N.A.Zhuk, M.G.Krzhizhanovskaya, N.A.Sekushin, D.V.Sivkov, I.E.Abdurakhmanov, Crystal structure, dielectric and thermal properties of cobalt doped bismuth tantalate pyrochlore, *J. Mater. Res. Technol.*, **22**(2023), 1791–1799. DOI:10.1016/j.jmrt.2022.12.059

[17] R.D.Shannon, Revised effective ionic radii and systematic studies of interatomic distances in halides and chalcogenides, *Acta Crystallogr. A.*, **32**(1976), 751–767.

[18] R.Grissa, H.Martinez, S.Cotte, J.Galipaud, B.Pecquenard, F.L.Cras, Thorough XPS analyses on overlithiated manganese ,spinel cycled around the 3V plateau, *Appl. Surface Science*, **411**(2017), 449–456. DOI: 10.1016/j.apsusc.2017.03.205

[19] M.A.Stranick, Mn2O3 by XPS., *Surface Science Spectra*, **6**(1999), 39–46.

[20] F.Gri, L.Bigiani, A.Gasparotto, C.Maccato, D.Barreca, XPS investigation of F-doped MnO_2 nanosystems fabricated by plasma assisted-CVD, *Surface Science Spectra*, **25**(2018), 024004. DOI: 10.1116/1.5048908

[21] F.Khairallah, A.Glisenti, XPS Study of MgO Nanopowders Obtained by Different Preparation Procedures, *Surface Science Spectra*, **13**(2006), 58–71. DOI: 10.1116/11.20060601

[22] N.A.Zhuk, M.G.Krzhizhanovskaya, A.V.Koroleva, etc., Cu, Mg codoped bismuth tantalate pyrochlores: crystal structure, XPS spectra, thermal expansion and electrical properties, *Inorg. Chem.*, **61**(2022), 4270–4282. DOI:10.1116/11.20060601

NEXAFS и XPS спектры марганецсодержащих пирохлоров на основе танталата висмута-магния

Надежда А. Жук
Сыктывкарский государственный университет имени Питирима Сорокина
Сыктывкар, Российская Федерация
Сергей В. Некипелов
Физико-математический институт Коми научного центра УрО РАН
Сыктывкар, Российская Федерация
Александра В. Королева
Санкт-Петербургский государственный университет
Санкт-Петербург, Российская Федерация
Алексей М. Лебедев
Национальный исследовательский центр – Курчатовский институт
Москва, Российская Федерация
Дмитрий С. Безносиков
Федеральное государственное унитарное предприятие «Главный радиочастотный центр»
Сыктывкар, Российская Федерация

Аннотация. По данным рентгенофазового анализа, синтезированные по керамической технологии образцы $Bi_2Mg_xMn_{1-x}Ta_2O_{9.5-\Delta}$ (x=0.3;0.5;0.7) содержат основную фазу кубического пирохлора (пр.гр. Fd-3m) и примесную фазу $BiTaO_4$ триклинной модификации (пр.гр. P-1), содержание которой пропорционально степени допирования марганцем. Параметр элементарной ячейки фазы пирохлора равномерно увеличивается с ростом индекса x(Mg) от 10.4970(8) при x=0.3 до 10.5248(8) Å (x=0.7), подчиняясь правилу Вегарда. Методом рентгеновской спектроскопии исследовано электронное состояние всех ионов, входящих в состав $Bi_2Mg_xMn_{1-x}Ta_2O_{9.5-\Delta}$. По данным NEXAFS и XPS установлено, что допирование магнием не изменяет степени окисления висмута и тантала в пирохлоре. Между тем, в $Ta4f_{-}$, $Bi4f_{7/2}$ и $Bi4_{f5/2}$ спектрах образцов наблюдается энергетический сдвиг полос поглощения в сторону меньших энергий, что характерно для ионов висмута и тантала с эффективным зарядом (+3-δ) и (+5-δ), обусловленных распределением ионов марганца(II) и магния(II) в позиции висмута и тантала. По данным NEXAFS и XPS спектроскопии, ионы марганца в образцах имеют степени окисления преимущественно +2 и +3, доля которых возрастает с увеличением содержания марганца в образцах.

Ключевые слова: пирохлор, Mg допирование $BiTaO_4$, XPS и NEXAFS спектроскопия.